



Available online at www.academicpaper.org

Academic @ Paper

International Journal of Energy
Applications and Technologies

Vol. 3, Issue 2, pp. 87 – 92, 2016



www.academicpaper.org/index.php/IJEAT

Research Article

MINI-SCALED HORIZONTAL AXIS WIND TURBINE ANALYSIS BY QBLADE AND CFD

Emre Koç¹, Onur Günel², Tahir Yavuz^{1*}

¹Baskent University Mechanical Engineering Department, Ankara, Turkey

²Yildirim Beyazit University Mechanical Engineering Department, Ankara, Turkey

Received 16th December 2016, Accepted 18th December 2016

Abstract

Abstract— The software QBlade under General Public License is used for analysis and design of wind turbines. QBlade uses the Blade Element Momentum (BEM) method for the simulation of wind turbines and it is integrated with the XFOIL airfoil design and analysis. It is possible to predict wind turbine performance with it. Nowadays, Computational Fluid Dynamics (CFD) is used for optimization and design of turbine application. In this study, Horizontal wind turbine with a rotor diameter of 2 m, was designed and objected to performance analysis by QBlade and Ansys-Fluent. The graphic of the power coefficient vs. tip speed ratio (TSR) was obtained for each result. When the results are compared, the good agreement has been seen.

Keywords- *QBlade, Computational Fluid Dynamics (CFD), Horizontal wind turbine, Blade Element Momentum (BEM), Wind Energy.*

1. Introduction

The importance of the renewable energy sources gradually increases with climate change. One of the renewable energy sources is the wind. Nowadays, the numbers of the green energy systems are increasing day by day and also, the small-scaled wind turbine are designed for the purpose of using at the greenhouse. Generally, two types of wind turbine are used. One is horizontal wind turbine and another is vertical wind turbine.

Also, the countries' economic growth is shown parallelism with the amount of the generated energy. In order to resume economic growth, the amount of the generated energy should be increased.

The energy sources based on fossil fuel increases carbon dioxide emission, therefore, studies on alternative energy source like wind and sun are continued.

Fig. 1 (a) is shown that, the amount of the generated energy from wind energy is approximately 432.88 GW until December 2015. Fig. 1 (b) is shown that new

wind energy power system having capacity of 63.467 GW was installed in 2015 [1].

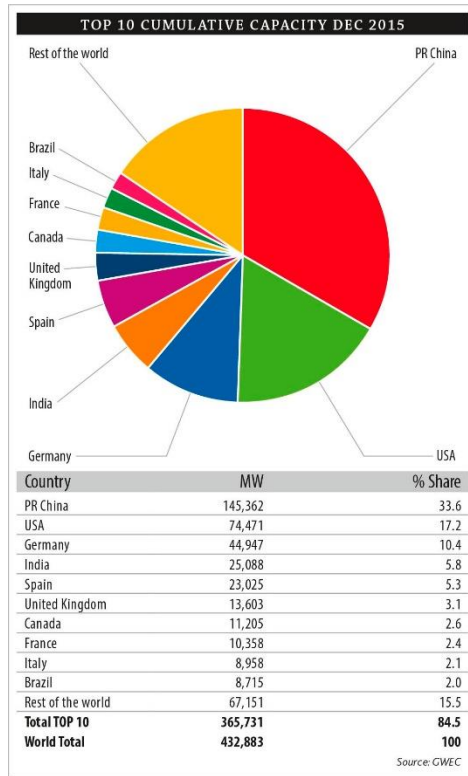
Wind turbine can be classified as large, medium, small and small-scaled. Large wind turbines have 50-100 m rotor diameter and they generate energy between 1 to 3 MW. Medium wind turbines have 20-50 m rotor diameter and they generate energy between 100 kW to 1 MW. Small wind turbines have 10-20 m rotor diameter and they generate energy between 25 kW to 100 kW. Small-scaled wind turbines can be separated three different types as micro, mini and household. Micro-scale wind turbines have 0.5-1.25 m rotor diameter and they generate energy between 0.004 kW to 0.25 kW. Mini-scale wind turbines have 1.25-3 m rotor diameter and they generate energy between 0.25 kW to 1.4 kW. Household wind turbines have 3-10 m rotor diameter and they generate energy between 1.4 kW to 16 kW [1].

It is possible to predict aerodynamic performance of wind turbine by using experimental, Computational Fluid Dynamics (CFD) and Blade Element Momentum (BEM) methods. Experimental and Computational Fluid Dynamics (CFD) methods are more expensive and require longer time than Blade Element Momentum (BEM) method. But, BEM method has less accuracy than experimental and CFD methods due to some assumption.

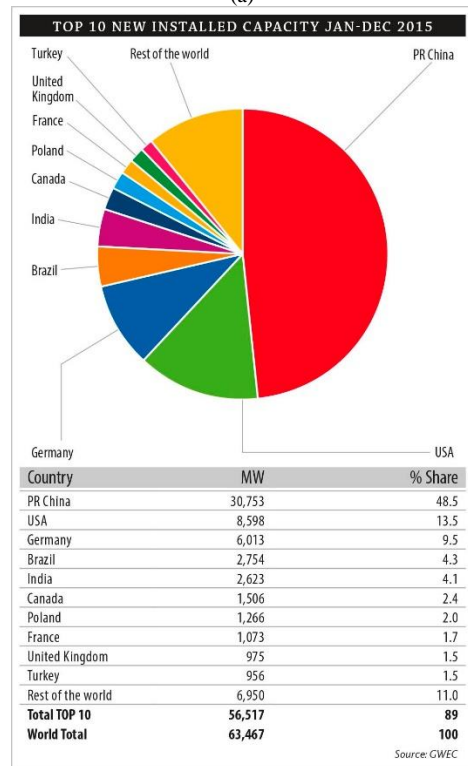
* Corresponding Authors;

tyavuz@baskent.edu.tr

Note: This paper has been presented at the International Conference on Advanced Technology & Sciences (ICAT'16) held in Konya (Turkey).



(a)



(b)

Fig. 1. (a) Cumulative capacity of wind turbines in 2015 around the world (b) New installed wind turbine capacity in 2015.

In this paper, for the horizontal wind turbine with a rotor diameter of 2 m, the aerodynamic performance is predicted by using QBlade and Ansys-Fluent. Firstly, the turbine is designed and aerodynamic performance is obtained by the software QBlade under

General Public License. After that, the 3D model of turbine is generated by using CATIA. Domain construction and grid generation for calculating the 3D wind turbine performance is described. Then, the aerodynamic performance is calculated by using CFD methods (Fluent commercial software). Finally, power curve and torque curve of the turbine obtained by the 3D CFD results, are compared with Qblade results.

2. QBLADE and CFD Analyses

Blade Element Momentum Method

Blade element momentum (BEM) theory is widely used in aerodynamic performance predictions and design applications for wind turbines. This theory combines both momentum theory and blade element theory methods. Momentum theory is useful to predict for ideal efficiency and flow velocity. Forces acting on the rotor to produce the motion of the fluid is determined by the mean of momentum theory. Momentum theory does not depend on the blade geometry. However, blade element theory depends on the blade geometry and it determines the forces acting on the blade after the motion of fluid. If these two theories are combined BEM theory, known as strip theory, is obtained and BEM theory defines the relation of rotor performance to rotor geometry. It is necessary to make assumption for the blade element theory and momentum theory.

For momentum theory:

- Blade operate without frictional drag
- A slipstream that is well defined separates the flow passing through the rotor disc from that outside disc
- The static pressure in and out of the slipstream far ahead of and behind the rotor are equal to the undisturbed free-stream static pressure
- Thrust loading is uniform over the rotor disc
- No rotation is imparted to the flow by the disc

For blade element theory:

- There is no interference between successive blade elements along the blade
- Forces acting on the blade element are solely due to the lift and drag characteristics of the sectional profile of a blade element [2].

The tangential and normal force coefficients in wind turbines can be calculated as the following:

$$C_T = C_L \sin \varphi - C_D \cos \varphi \quad (1)$$

and

$$C_N = C_L \cos \varphi + C_D \sin \varphi \quad (2)$$

BEM theory equations can solved as iteratively. There are two iterative variables that are axial and radial induction factors, in BEM theory. These variables can be defined as follows [3].

$$a = \frac{1}{\frac{4 \sin^2 \phi}{(\sigma C_N)} + 1} \quad (3)$$

$$a' = \frac{1}{\frac{4 \sin \phi \cos \phi}{(\sigma C_T)} - 1} \quad (4)$$

where, ϕ is the inflow angle, C_T and C_N is the tangential and normal force coefficient respectively, σ is the solidity which is defined as the ratio of the planform area of the blades to the swept area [4]. It can be expressed as follows:

$$\sigma = \frac{cB}{2\pi r} \quad (5)$$

where, c is the chord length, B is the number of blades and r is the disk radius.

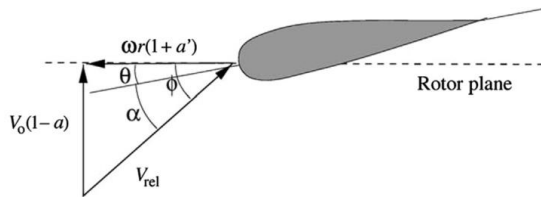


Fig.2. Velocity component in the rotor plane [5].

Fig.2 shows the velocity component in the rotor plane. If the axial and radial induction factors are firstly guessed, the inflow angle, ϕ , can be computed. Then, the angle of attack α , that is the between the chord line of the airfoil and the relative wind speed, can be obtained by using the following equation:

$$\theta = \theta_p + \beta \quad (6)$$

$$\alpha = \phi - \theta \quad (7)$$

where β is a twist angle of the blade, θ_p is a pitch angle of the blade, θ is the combination of the twist angle β and the pitch angle θ_p . After the calculation of the angle of attack, the lift and drag coefficient of the airfoil can be obtained from the lift and drag curves of the airfoil. By using these force coefficients, new induction factors can be calculated and compared to the initial induction factors. When the maximum value of the Δa and $\Delta a'$ is below the convergence criterion ϵ , it means that the iteration converge. Then, the next element can be calculated.

The flow diagram, which is used to solve iteratively for Axial Induction Factor and the Radial Induction Factor solution of BEM theory is shown in Fig 3.

Blade Shape Design for Optimum Rotor with Wake Rotation

When an ideal rotor is design, the effect of wake rotation is taken into design. The blade shape optimization for ideal rotor includes wake rotation except drag ($C_D = 0$) and tip losses ($F = 1$). The power

coefficient depends on the angle of the inflow angle, ϕ . The power coefficient can be obtained from the following equation:

$$C_p = \left(\frac{8}{\lambda^2}\right) \int_{\lambda_h}^{\lambda} \sin^2 \phi (\cos \phi - \lambda_r \sin \phi) (\sin \phi + \lambda_r \cos \phi) [1 - (C_d/C_l) \cot \phi] (\lambda_r)^2 d\lambda_r \quad (8)$$

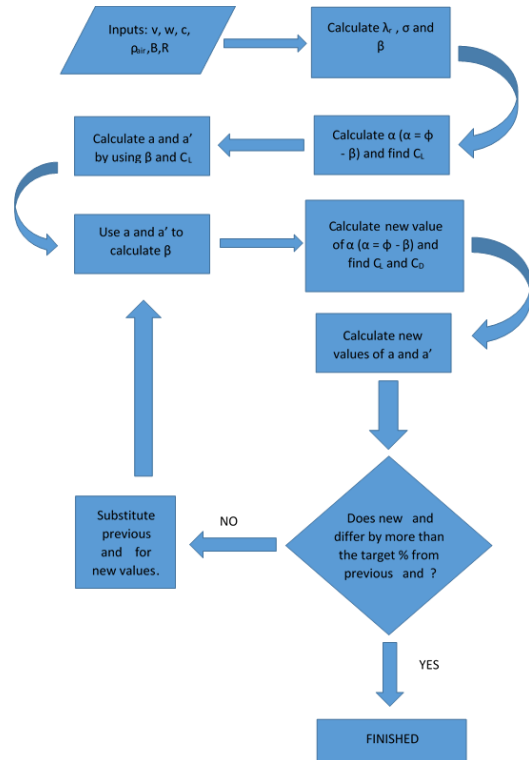


Fig. 3. Flow Diagram of the Iteration Process Used to Solve for Axial Induction Factor and the Radial Induction Factor.

Taking the partial derivative of the part of the integral for C_p and the derivative is set to equal zero.

$$\frac{\partial}{\partial \phi} [\sin^2 \phi (\cos \phi - \lambda_r \sin \phi) (\sin \phi + \lambda_r \cos \phi)] = 0 \quad (9)$$

The local tip speed ratio, inflow angle, chord length of the blade section can be calculated as the follows:

$$\lambda_r = \sin \phi (2 \cos \phi - 1) / [(1 - \cos \phi)(2 \cos \phi + 1)] \quad (10)$$

$$\phi = (2/3) \tan^{-1}(1/\lambda_r) \quad (11)$$

where λ_r is the local tip speed ratio, c is the chord length of the blade section, B is the number of the blade, C_L is lift coefficient at the angle of the attack, α which the angle is at the highest value of the ratio of the lift-drag coefficient.

For an ideal wind turbine blade design, firstly it was decided to design a 2 m blade diameter turbine. SG6043 airfoil type which is designed exclusively for wind turbines with small blades [6] was selected. Tip speed ratio, λ , was chosen 5. For SG6043 airfoil, the lift coefficient at the angle of attack 4.5° , where the C_L/C_D ratio has maximum rate, was acquired as 1.22 from Xflr5 software. Blade section was divided 9

parts. Then from the formulas inflow angle, chord length and twist angle were calculated for each section.

The rotor blades parameter and the design parameter of wind turbine is listed in Table 1 and Table 2, respectively.

Table 1. The parameter of the rotor blades.

Blade	
Radius of blade (m)	1
Number of the blades	3
Airfoil types	SG6043
Chord length (m)	Listed in Table 2.
Twist angle (deg)	Listed in Table 2.

Table 2. Design parameter of blade.

Geometry of Blade			
Section	r/R	Chord length (m)	Twist angle (deg)
1	0.2	0.184	25.50
2	0.3	0.156	17.96
3	0.4	0.130	13.21
4	0.5	0.110	10.03
5	0.6	0.094	7.79
6	0.7	0.082	6.13
7	0.8	0.073	4.86
8	0.9	0.066	3.85
9	1	0.059	3.04

The SG6043 airfoil, has a maximum thickness of % 10, a camber of 5.5 % and a leading edge radius of 1.7 %. The profile is shown in Fig. 4. Also blade model of turbine is shown in Fig 5.

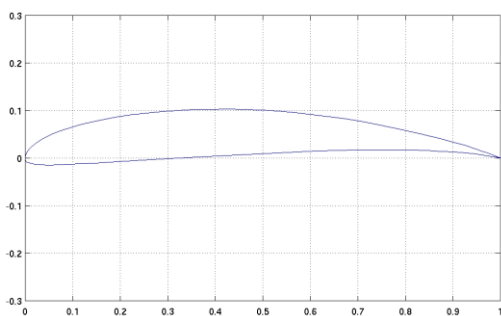


Fig. 4. SG6043 airfoil profile.

Qblade Analysis

Qblade analyses were conducted on the turbine blade in the range of the tip speed ratio, λ from 2.5 to 6.5. In the analyses design velocity of 12 m/s was kept to be constant while the rotation of the rotor was varied with respect to λ . As results, the power coefficient and torque values vs. various tip speed ratio graphics were obtained (Fig. 6, Fig. 7).

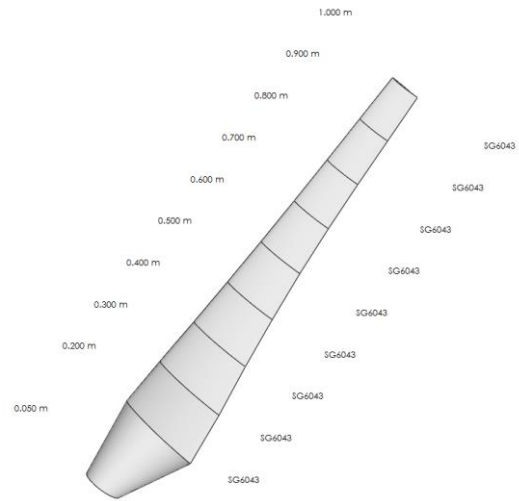


Fig.5. Blade model of wind turbine.

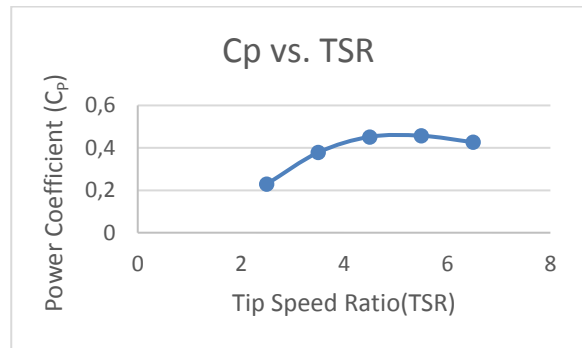


Fig. 6. The power coefficient versus tip speed ratio graphic in Qblade.

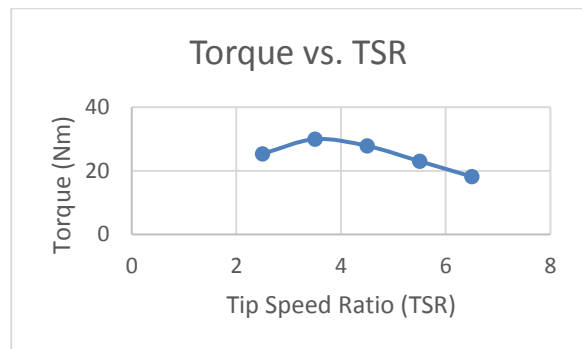


Fig. 7. Torque versus tip speed ratio graphic in Qblade.

CFD Analysis

Numerical simulations for aerodynamic performance of wind turbine were carried out by using Ansys-Fluent, which is commercial software for CFD analysis based on the finite volume method. In CFD analysis, SST k- ω turbulence module with curvature correction for Reynolds-average Navier-Stokes (RANS) equation was used. Also, second-order upwind discretization in space was used. The convergence rate was monitored during the iteration process by means of the residuals of the dependent variables of the governing differential equations.

Wind turbine module shown in Fig. 8 was obtained using CATIA, commercial software for 3D CAD design.

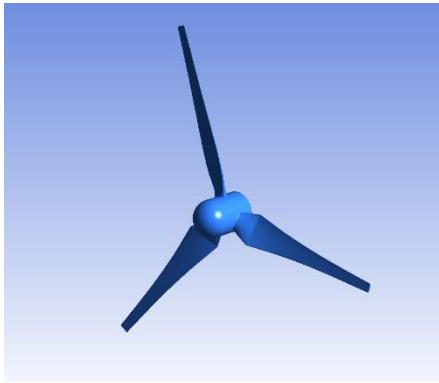


Fig. 8. 3D Wind Turbine model.

The external domain, which is a rectangular parallelepiped of width 6 m, length 15 m, height 6 m, is shown in Fig. 9. Domain entrance was defined as “Velocity Inlet” and exit was defined as “Pressure Outlet” boundary conditions. The outer domain's walls were defined as “Symmetry” boundary condition. A cylindrical domain which is connected to external domain was also created around the blades. Moving Reference Model (MRF) was used for this cylinder domain to give blade rotation.

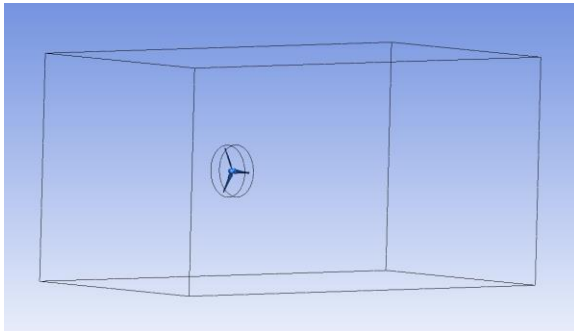


Fig. 9. The Flow domain with 6 m x 6 m x 15 m dimensions for 3D analysis.

The unstructured grid was applied on the turbine rotating disk area and external flow domain surrounding the turbine. The conformal grid was used on the interface between the rectangular external flow domain and cylindrical rotating disk domain. Different size of grids was used to obtain grid independency of the analysis results. This is achieved by obtaining solutions with increasing number of grid nodes until a stage is reached where the solution exhibits negligible change with further increase in the number of nodes. The grid structure is shown in Fig. 10.

In order to resolve the boundary layer, 25 layers in the boundary were introduced and first layer was located 0.015 mm from the wall. Hence, the first grid point off the wall in the normal direction was placed at a distance less than $y^+=3$ from the wall. The y^+ ($\rho U_{\tau} y / \mu$) is defined as the non-dimensional wall distance for wall-bounded flow in a turbulent

boundary layer analysis. To consider the viscous sublayer in the turbulent boundary layer, the value of the y^+ has to be less than 10 [7, 8].

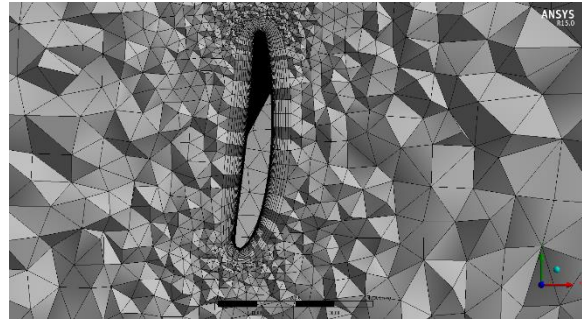


Fig. 10. The grid structure of the flow domain.

After the CFD analysis, obtained distribution of the y^+ plus on the blades is shown in Fig 11.

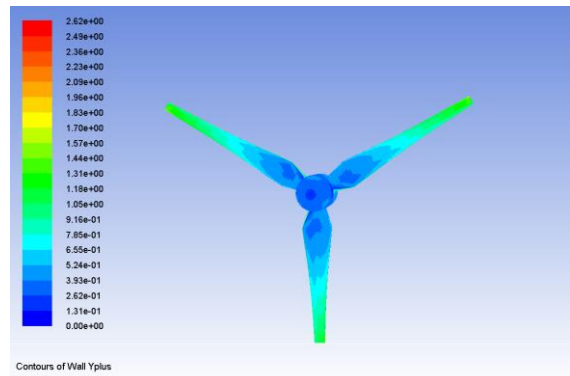


Fig. 11. Contour of y^+ plus distribution on the blades.

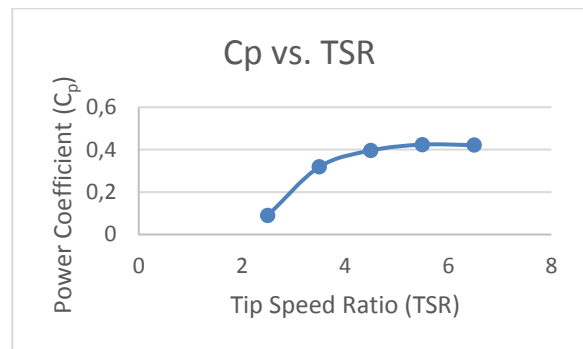


Fig. 12. The power coefficient versus tip speed ratio graphic in Fluent.

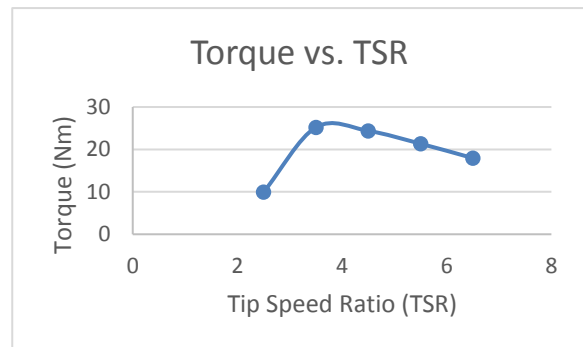


Fig. 13. Torque versus tip speed ratio graphic in Fluent.

Based on 12 m/s of design wind speed, horizontal axis wind turbine performance analyses were performed by using Ansys-Fluent software. As results, the power coefficient and torque values vs. various tip speed ratio graphics were obtained (Fig. 12, Fig. 13).

3. Conclusions

This study was considered the performance characteristics of the wind turbine, which has SG6043 airfoil. The commercial code Fluent with SST $k-\omega$ and the general public license QBlade, which uses BEM theory to predict aerodynamic coefficients, were used respectively. The following conclusions were drawn; Xflr5 software was used to obtain the values of the angle where C_L/C_D ratio has maximum and max. C_L at this angle of attack. These values were obtained as 4.5° and 1.22 respectively. Maximum torque value was obtained as 29.937 Nm in Qblade and 25.204 Nm in Fluent at the tip speed ratio of 3.5. Maximum power coefficient value was obtained as 0.457 in Qblade and 0.424 in Fluent at the tip speed ratio 5.5.

The efficiency of the system first increases and reaching to maximum value and then decreases with increasing the tip speed ratio.

There are reasonable agreements between Qblade and Fluent analyses. At high tip speed ratio value, the results get closer in Qblade and Fluent solutions (Fig. 14, Fig. 15).

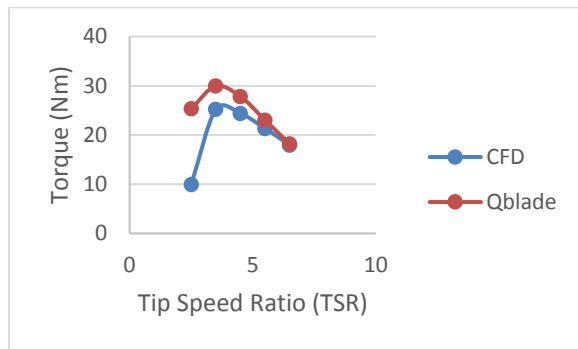


Fig. 14. Comparison of torques for wind turbine in Qblade and Fluent analyses.

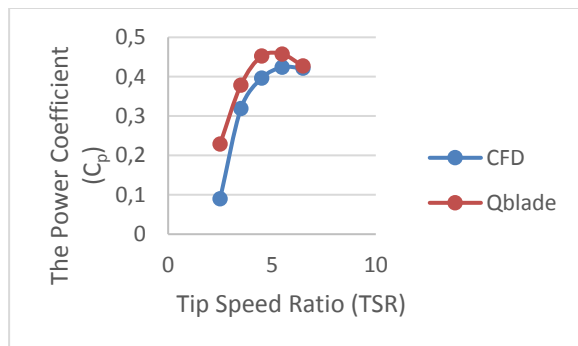


Fig. 15. Comparison of the power coefficients for wind turbine in Qblade and Fluent analyses.

References

- [1] (2015) The Global Wind Energy Council website. [Online] Available: <http://www.gwec.net/>
- [2] R. Wilson, P. Lissaman and S. Walker, Aerodynamic Performance of Wind Turbines, 1976.
- [3] V. Esfahanian, A. Salavati Pour, I. Harsini, A. Haghani, R. Pasandeh, A. Shahbazi, G. Ahmadi, "Numerical Analysis of Flow Field Around NREL Phase II Wind Turbine by a Hybrid CFD/BEM Method," J. Wind Eng. Ind. Aerodyn., 2013, pp. 29-36.
- [4] J. F. Manwell, J. G. Mcgowan, A. L. Rogers, "Wind Energy Explained Theory, Design and Application," Wiley, 2009.
- [5] M. O. L. Hansen, "Aerodynamics of Wind Turbines," 2nd. Ed. Earthscan, London, 2008.
- [6] P. Giguere, M. S. Selig, "New Airfoils for Small Horizontal Axis Wind Turbines," Solar Energy Engineering, 1998, pp. 108-114.
- [7] Hua X, Gu R, Jin J, Liu Y, Ma Y, Cong Q, et al. "Numerical Simulation And Aerodynamic Performance Comparison Between Seagull Airfoil and NACA 4412 Airfoil Under Low-Reynolds," Adv. Nat. Sci., Vol. 3, No. 2, 2010, pp. 244-250.
- [8] T. Yavuz, E. Koç, B. Kılış, Ö. Erol, Can Balas, T. Aydemir, "Performance analysis of the airfoil-slat arrangements for hydro and wind turbines applications," Renew. Energy, 74 (414), 2015, pp. 414-421.